

REGULARIZED DEQUANTIZER FOR MPEG

Gunho Lee, Sung-Jea Ko, *Senior Member, IEEE*, Sanghoon Sull,
Member, IEEE and Samuel Moon-Ho Song, *Member, IEEE*
 School of Electrical Engineering, Korea University
 Sungbuk-gu Anam-dong 5 Ga 1
 Seoul 136-701, Korea

ABSTRACT

Based on regularization principles, we propose a new dequantization scheme for MPEG. The new approach drastically reduces blocking artifacts without smoothing the decoded image. Most discrete cosine transform (DCT) based video coding suffer from blocking artifacts where boundaries of 8×8 DCT blocks become visible on decoded images. The blocking artifacts become more prominent as the bit rate is lowered. In this paper, we present a new dequantization technique for discrete cosine transform (DCT) based encoding to sharply reduce the blocking artifacts. Our proposed dequantization scheme, through regularization, sharply reduces blocking artifacts in decoded images. The performance of the proposed algorithm will be evaluated against the standard MPEG decoding. The comparison will show visual improvements as well as numerical improvements in terms of the peak-signal-to-noise ratio (PSNR) and the blockiness measure (BM) to be defined.

1. INTRODUCTION

Emergence of internet video as well as high definition television has been fueling the recent surge in digital video related research. In particular, the international standard MPEG for compression of digital video has received much attention due to the fact that it is an open standard for any developers as well as researchers. In this paper, we propose a slightly different dequantization scheme (an improved decoder), which will work with the standard MPEG compressed video. The proposed dequantizer will be shown to be superior over the currently specified dequantization scheme.

Several investigators have recently reported algorithms dealing with the quantization matrix and the associated dequantization scheme. In [1], Prost, *et al.* proposes a technique that modifies the quantization matrix to be used by the decoder. That is, the encoder uses one quantization matrix while the decoder uses a different quantization matrix. The new quantization matrix, used during decoding, is computed (by the encoder) using an approach similar to Miller's least squares solution [2] for image restoration applications [3]. The solution proposed in [1], and later corrected by Philips [4], offers a dequantization scheme different from the standard method.

Konstantinides, *et al.* [5] propose yet another technique for computing a modified quantization matrix for image sharpening applications directly in DCT domain. However, neither approaches [1,5] guarantee that the dequantization process will map the quantized DCT coefficients to its value \pm (quantizer spacing/2) in DCT domain.

In contrast, we propose a regularization based dequantizer which will guarantee the mapping of quantized DCT coefficients to within \pm (quantizer spacing/2). This is guaranteed through a built-in non-linearity in our proposed iterative algorithm.

2. FORMULATION

2.1 Modeling DCT-based Transform Coding

Before dealing with details of the regularized dequantization, the conventional DCT-based transform coding currently specified in the MPEG standard (as well as JPEG, H.261 and H.263) is reviewed to establish the notation.

In MPEG or other conventional DCT-based transform coding standards, the image is first divided into 8×8 blocks and the individual blocks are transformed by the discrete cosine transform (DCT). We denote the output of this operation by \mathbf{Df} , where \mathbf{f} is the lexicographically ordered image and the operator \mathbf{D} is the appropriately defined 2-D DCT matrix. The DCT coefficients are then quantized with or without a dead-zone. Since the quantization process includes a division (or a multiplication by its inverse) step by elements of the quantization matrix, the quantization operator \mathcal{Q} can be mathematically expressed as follows:

$$\begin{aligned} \mathcal{Q}\{\mathbf{Df}\} &= \text{round}\{\mathbf{M}^{-1}\mathbf{Df} - \text{sgn}(\mathbf{Df})\delta/2\} \\ &= \mathbf{M}^{-1}\mathbf{Df} - \text{sgn}\{\mathbf{Df}\}\delta/2 + 1/2 \\ &\quad - \text{rem}\{\mathbf{M}^{-1}\mathbf{Df} - \text{sgn}(\mathbf{Df})\delta/2 + 1/2\} \end{aligned} \quad (1)$$

where $\text{round}\{\}$ and $\text{rem}\{\}$ operators indicate the usual rounding and remainder operations, respectively; and $\text{sgn}\{\}$ is the signum function that maps positive, zero and negative valued reals to 1, 0 and -1 , respectively. Furthermore, \mathbf{M} is a diagonal matrix whose elements consist of appropriately ordered elements of the quantization matrix. Note that $\delta = 1$ for quantization with a dead-zone. If we let $\delta = 0$, Eq. (1) then represents quantization without a dead-zone. Lastly, we have also used the identity:

$$\text{round}\{x\} = x + 1/2 - \text{rem}\{x + 1/2\}. \quad (2)$$

The quantized DCT coefficients are then encoded losslessly.

Upon receipt of losslessly encoded quantized DCT coefficients, the decoder first reverses the lossless encoding process to obtain quantized DCT coefficients. The lossless encoding and decoding steps together form a mathematical identity and thus, we neglect this part in the current development. In any case, the decoder has access to quantized DCT coefficients $\mathcal{Q}\{\mathbf{Df}\}$ as

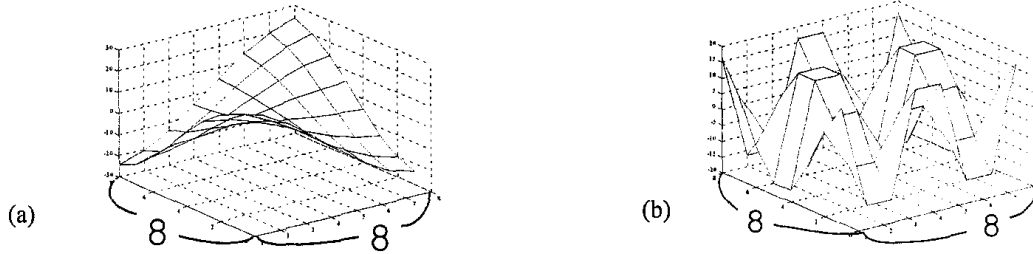


Figure 1: The quantization error introduced by the ij^{th} DCT coefficient represented in the spatial domain (the c_{ij} matrix). (a) c_{11} and (b) c_{24} . The quantization error introduced by the ij^{th} DCT coefficient manifests itself as a spatially varying error (except for the DC coefficient where it would cause a constant error within the 8×8 block).

computed by the encoder. The dequantization operation P can simply be modeled by a multiplication by \mathbf{M} , quantization followed by a correction for dead-zones. That is,

$$\begin{aligned} P\{Q\{\mathbf{Df}\}\} &= \mathbf{M}\{Q\{\mathbf{Df}\} + \text{sgn}\{\mathbf{Df}\}\delta/2\} \\ &= \mathbf{Df} + \mathbf{M}\{1/2 - \text{rem}\{\mathbf{M}^{-1}\mathbf{Df} - \text{sgn}\{\mathbf{Df}\}\delta/2 \\ &\quad + 1/2\}\} \end{aligned} \quad (3)$$

Again, in the above, $\delta = 1$ indicates quantization with a dead-zone and $\delta = 0$ without a dead-zone.

The conventional decoder then takes the dequantized DCT coefficients and performs the 2-D inverse discrete cosine transform (IDCT) as follows:

$$\begin{aligned} \mathbf{g} &= \mathbf{D}^{-1}PQ\{\mathbf{Df}\} \\ &= \mathbf{f} + \mathbf{D}^{-1}\mathbf{M}\{1/2 - \text{rem}\{\mathbf{M}^{-1}\mathbf{Df} - \text{sgn}\{\mathbf{Df}\}\delta/2 \\ &\quad + 1/2\}\} \end{aligned} \quad (4)$$

Note that what is desired is the original image \mathbf{f} ; however, the image as determined by the conventional decoder is \mathbf{g} . This conventionally decoded image includes the quantization error which precisely is the second term of Eq. (4):

$$\text{error} = \mathbf{D}^{-1}\mathbf{M}\{1/2 - \text{rem}\{\mathbf{M}^{-1}\mathbf{Df} - \text{sgn}\{\mathbf{Df}\}\delta/2 + 1/2\}\} \quad (5)$$

It is important to note that the quantization error originally introduced in the DCT domain (by the rounding operation of Eq. (1), has been re-expressed in the spatial domain. In other words, Eq. (5) is exactly the quantization error expressed in the spatial domain.

Direct interpretation of the derivation leading to Eq. (5) results in the following. The quantization error as shown in Eq. (5) above is due to the quantization Q followed by the conventional dequantization described by Eq. (3). The natural question to ask is whether there exists a better dequantizer. Without any further information regarding the image, and because the error term above depends on the original image \mathbf{f} , using the conventional dequantizer (3) appears to be the only choice. However, through regularization, with the assumption that the image \mathbf{f} is smooth, we have developed a different dequantization procedure.

In view of the inequality

$$-1/2 < 1/2 - \text{rem}(x + 1/2) \leq 1/2. \quad (6)$$

The error in the DCT coefficients (just before the IDCT step) also obey

$$\begin{aligned} &|\mathbf{e}_n^T \mathbf{M}\{1/2 - \text{rem}\{\mathbf{M}^{-1}\mathbf{Df} - \text{sgn}\{\mathbf{Df}\}\delta/2 + 1/2\}\}| \\ &\leq \frac{\mathbf{e}_n^T \mathbf{M} \mathbf{e}_n}{2}, \quad \text{for all } n \end{aligned} \quad (7)$$

where T indicates transpose and \mathbf{e}_n is the Euclidean basis vector with a "1" in the n th row and zeros in other rows. Although Eq. (7) appears to be cumbersome, what it states is simply that, the error introduced (in DCT domain) by the quantizer is limited between \pm (quantizer spacing/2) for n th DCT coefficient. This observation allows a slightly different relationship between \mathbf{g} and \mathbf{f} . For this purpose, define:

$$c_{ij} = 2\text{D-IDCT of } \begin{bmatrix} 0 & \dots & 0 & 0 & 0 & \dots & 0 \\ \vdots & & \vdots & \vdots & \vdots & & \vdots \\ \vdots & & 0 & 0 & 0 & & \vdots \\ 0 & \dots & 0 & q_{ij} & 0 & \dots & 0 \\ \vdots & & 0 & 0 & 0 & & \vdots \\ \vdots & & \vdots & \vdots & \vdots & & \vdots \\ 0 & \dots & 0 & 0 & 0 & \dots & 0 \end{bmatrix} \quad (8)$$

where q_{ij} is the ij^{th} element of the quantization matrix. Furthermore, let \mathbf{c}_y be lexicographically ordered version of c_{ij} . Then,

$$\mathbf{g}(k) = \mathbf{f}(k) + \sum_{0 \leq i, j < 7} \alpha_{ij}(k) \mathbf{c}_y \quad (9)$$

where the argument (k) indicates the extraction of the corresponding k th 8×8 block. Thus, all vectors in Eq. (9) are of the size 64×1 . Furthermore, due to the inequality as shown by Eq. (7), the coefficients $\alpha_{ij}(k)$ are restricted to lie within the interval $(-1/2, 1/2]$. Note that Eq. (9) is satisfied for all

8×8 blocks of the image. This is true whether or not the dead-zone is used by the quantizer.

The following observations may be made regarding the matrix c_{ij} . Firstly, it is precisely the i^{th} basis vector for the inverse DCT. Secondly, it is the quantization error introduced by the i^{th} DCT coefficient represented in the spatial domain. In other words, the quantization error introduced by the i^{th} DCT coefficient manifests itself as a spatially varying error (except for the DC coefficient where it would cause a constant error within the 8×8 block) represented by c_{ij} . Figure 1 shows the matrices (a) c_{11} and (b) c_{24} . Note that the matrices c_{11} and c_{24} show the spatial quantization error caused by the DCT coefficients (1,1) and (2,4), respectively.

2.2 Regularization

In view of the previous analysis, the question that we pose is: find $\alpha_{ij}(k)$ to minimize $\| \mathbf{f} - \mathbf{g} \|_2$, the L_2 -norm, using Eq. (9). The problem as stated is an *ill-posed problem* [6], and a unique solution cannot be obtained. The remedy is to regularize the problem. By assuming that the original image $f(x, y)$ is "smooth", we solve: find f that minimizes:

$$\| f - g \|_2^2 + \lambda \| \nabla f \|_2^2 \tag{10}$$

The minimizer of the functional in Eq. (10) obeys the following Euler-Lagrange Equation [7]:

$$F_f - \frac{\partial}{\partial x} F_{f_x} - \frac{\partial}{\partial y} F_{f_y} = 0 \tag{11}$$

where $F = (f - g)^2 + \lambda(f_x^2 + f_y^2)$ and subscripts indicate partial differentiation along the direction of the subscripting variable. Substitution of appropriate variables into the Euler-Lagrange Equation (11) results in the following Poisson Equation:

$$\nabla^2 f = \frac{1}{\lambda}(f - g) \tag{12}$$

with an appropriate boundary condition (Dirichlet or Neumann) depending on the particular application. Although for a different application, see [8] for a detailed description of the boundary condition in relation to the Euler-Lagrange Equation.

3. Image Decoding by Regularized Dequantizer

The decoded image must still be based on the received quantized DCT coefficients and thus must satisfy Eq. (9). Therefore, Eq. (12) cannot be used by itself. Because we are only interested in a dequantizer that modifies quantized DCT coefficients by \pm (quantizer spacing/2), Eq. (12) must be used together with Eq. (9).

The substitution of Eq. (9) into a lexicographically ordered version of Eq. (12) yields:

$$\sum_{0 \leq i, j \leq 7} \alpha_{ij}(k) (Lc_{ij} - \frac{1}{\lambda} c_{ij}) = Lg(k) \tag{13}$$

where L is the matrix representation of the Laplacian operator for lexicographically ordered operands (*i.e.*, vectors). Note that the original image \mathbf{f} has been completely eliminated in Eq. (13). In fact, all terms that appear in Eq. (13) are known except for the coefficients $\alpha_{ij}(k)$. Therefore, the problem at hand is to determine $\alpha_{ij}(k)$, using Eq. (13). For this purpose, Eq. (13) may be written in matrix-vector form as follows:

$$\left[Lc_{00} - \frac{1}{\lambda} c_{00} \mid \cdots \mid Lc_{77} - \frac{1}{\lambda} c_{77} \right] \alpha(k) = Lg(k) \tag{14}$$

where $\alpha(k)$ is the lexicographically ordered version of the coefficients $\alpha_{ij}(k)$. It can be shown that the system of equations above is invertible and it may be solved exactly and $\alpha(k)$ can be found simply by inverting Eq. (14). Certain fast FFT-like approaches may also be used. Note that Eq. (14) must be satisfied for all 8×8 blocks. Once $\alpha(k)$ has been determined for all blocks, the desired image can be obtained by Eq. (9) for all 8×8 blocks. However, because the coefficients $\alpha_{ij}(k)$ must be limited to lie in the interval $(-1/2, 1/2]$, we must resort to an iterative approach. In other words, if any of the computed coefficients $\alpha_{ij}(k)$ lies outside the interval $(-1/2, 1/2]$, those coefficients must be clipped. The algorithm then recomputes the coefficients based on the currently available data. The proposed iterative decompression algorithm including the regularized dequantizer is summarized below:

- Initialize image with the conventionally decoded image:
 $\mathbf{f}^{(0)} = \mathbf{g}$
- Initialize coefficients for all 8×8 blocks: $\alpha_{ij}(k) = 0$
- Loop for $m = 0, 1, 2, 3, \dots$
 - Find the incremental coefficient $\alpha_{ij}^{(m)}(k)$:
Solve Eq. (14) with $\mathbf{g} = \mathbf{f}^{(m)}$.
 - Update and clip the effective coefficient:
 $\alpha_{ij}(k) = \min(\max(\alpha_{ij}(k) + \alpha_{ij}^{(m)}(k), -1/2), 1/2)$
 - Update the current image (for all 8×8 blocks):
 $\mathbf{f}^{(m+1)}(k) = \mathbf{g}(k) - \sum_{0 \leq i, j \leq 7} \alpha_{ij}(k) c_{ij}$

The end result or the decoded image, is in effect, the IDCT of the regularized dequantizer output. In practice, the coefficients $\alpha_{ij}(k)$ corresponding to low frequency components rapidly grow to values outside the interval $(-1/2, 1/2]$, which is then clipped within the iteration loop. This clipping allows coefficients corresponding to higher frequency components to rise. In any case, because the final decoded image is based on Eq. (13) the proposed technique guarantees the updating of received DCT coefficients to within \pm (quantizer spacing/2) for all DCT coefficients.

The algorithm described above is a different dequantization scheme in comparison to other approaches described in various DCT-based coding standards, where the computed DCT coefficients are quantized according to the quantizer spacing

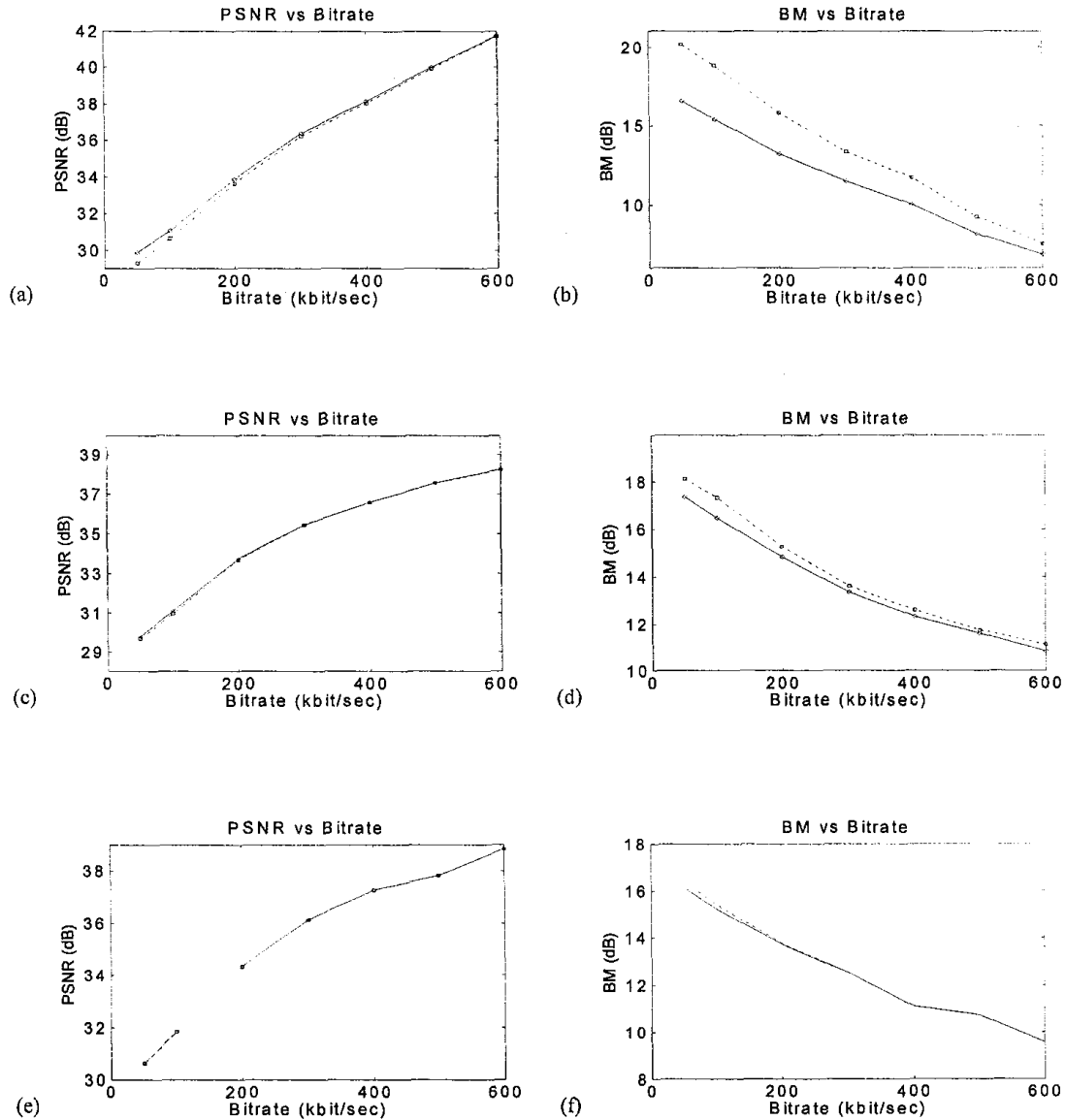


Figure 2: The PSNR—(a), (c), and (e)—and the BM (blockiness measure)—(b), (d) and (f)—as functions of the bitrate achieved by decompression using conventional MPEG decoder (dotted) and by decompression using the proposed regularized dequantizer. (a) and (b): for I-frame, (c) and (d): for P-frame and (e) and (f): for B-frame.

specified by the quantization matrix elements. As an instance, on the encoder side, suppose

- computed DCT coefficient = 41.2
- quantization matrix element for this particular coefficient = 8
- encoded data = 5 (= round { 41.2 / 8 })

Then, on the decoder side,

- received data = 5
- quantization matrix element for this particular coefficient = 8

$$\text{- reconstructed DCT coefficient} = 40 = 5 * 8$$

Note that in this particular case, the quantization error = 1.2 which is bounded to within \pm (quantizer spacing/2). Our proposed algorithm does not simply multiply the quantizer spacing to the received data, which in this case is 40. The proposed dequantizer will map the received data to within the range (36, 44), where the actual value is chosen so that the final decompressed image is "smooth" in the sense of minimizing the cost functional given in Eq. (10).

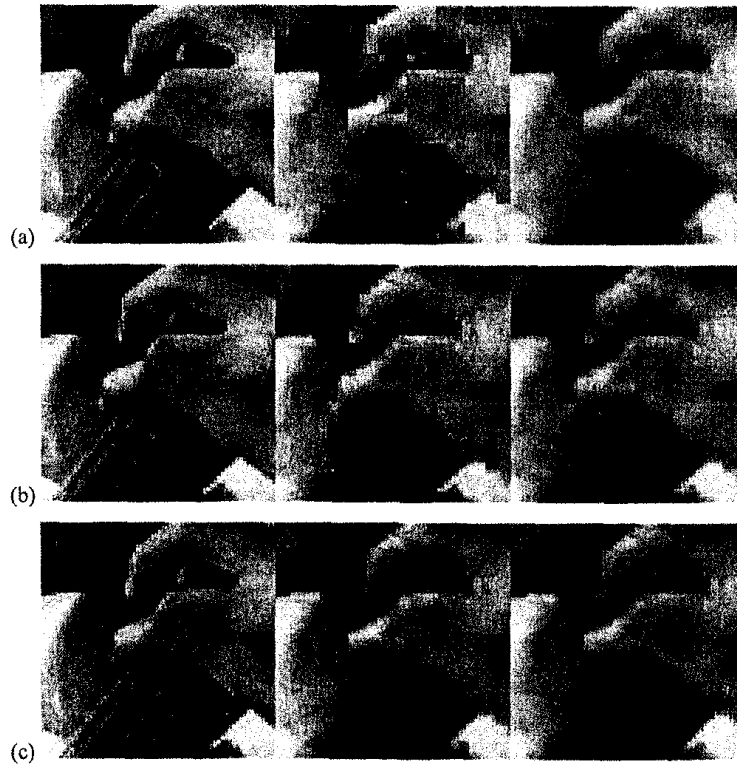


Figure 3: Zoomed images ($\times 2$) of the original (left), MPEG decomposition (center) and, decomposition by the proposed regularized dequantizer (right). (a): I-frame, (b): P-frame, and (c): B-frame. Note that the proposed regularized dequantizer based decoder out performs the conventional MPEG decoder for all frame types. The performance gain is most obvious for the I-frame. See Figure 2.

4. RESULTS

The performance of the proposed regularized dequantizer is evaluated and compared to the standard H.263+ with its standard quantization table with and without the deblocking filter (Annex J). The blockiness measure (BM) defined by the following will be used to compare the two approaches.

$$\text{BM} = 10 \log_{10} \left\{ \frac{\sum_{\text{vertical}} \left\| \frac{\partial}{\partial x} (f - \hat{f}) \right\|_2^2 + \sum_{\text{horizontal}} \left\| \frac{\partial}{\partial y} (f - \hat{f}) \right\|_2^2}{N_{\text{pix}}} \right\} \quad (15)$$

where N_{pix} is the total number of pixels summed. In the above, f is the original image and \hat{f} is the decompressed image by one of (i) MPEG, (ii) H.263+ decomposition, (iii) H.263+ with its deblocking filter and (iv) the proposed regularized dequantizer. Note that the differences in the

derivatives across the 8×8 block boundary are summed only along vertical and horizontal block boundaries. Higher BM indicates more severe blocking artifact.

Figure 2 (a) and (b) show PSNR and BM values for a typical I-frame; (c) and (d) for a P-frame; and (e) and (f) for a B-frame, all obtained in two iterations. Note that the improvement provided by the proposed regularized dequantizer for I frame is much greater than that of the P- and B-frames. Although improvements in actual PSNR values appear to be small (less than 1 dB for I-frame and almost negligible for B-frame) the improvements in BM values are more apparent for all frame types, especially for I-frame. In addition, a few trends can be observed from these plots. (1) The performance difference is most obvious for the I-frame and this difference is less prominent the P- and the B-frames. (2) The improvement in both the PSNR as well as BM becomes more relevant for low bit rates. (3) The improvement in the BM is greater than that of the improvement in PSNR for all frame types. (4) Higher performance gain can be expected for lower bit rate videos, however for extremely high bit rate videos, the performance gain will not be as obvious.

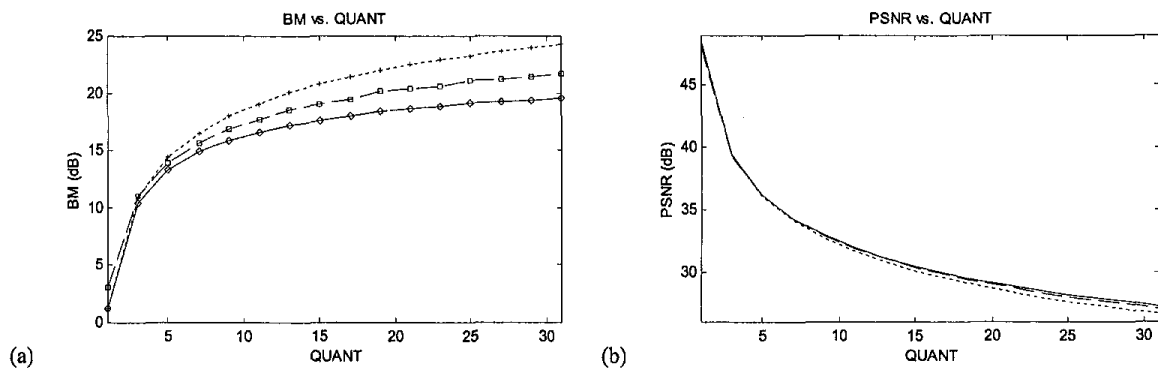


Figure 4: The PSNR and BM (blockiness measure) values obtained with the standard Lenna image: (a) PSNR and (b) BM as functions of QUANT (quantizer scale) for decompression using the conventional H.263+ decoder (dotted), H.263+ decoding followed by the deblocking filter of H.263+ Annex J (dashed), and by the proposed regularized dequantizer (solid).

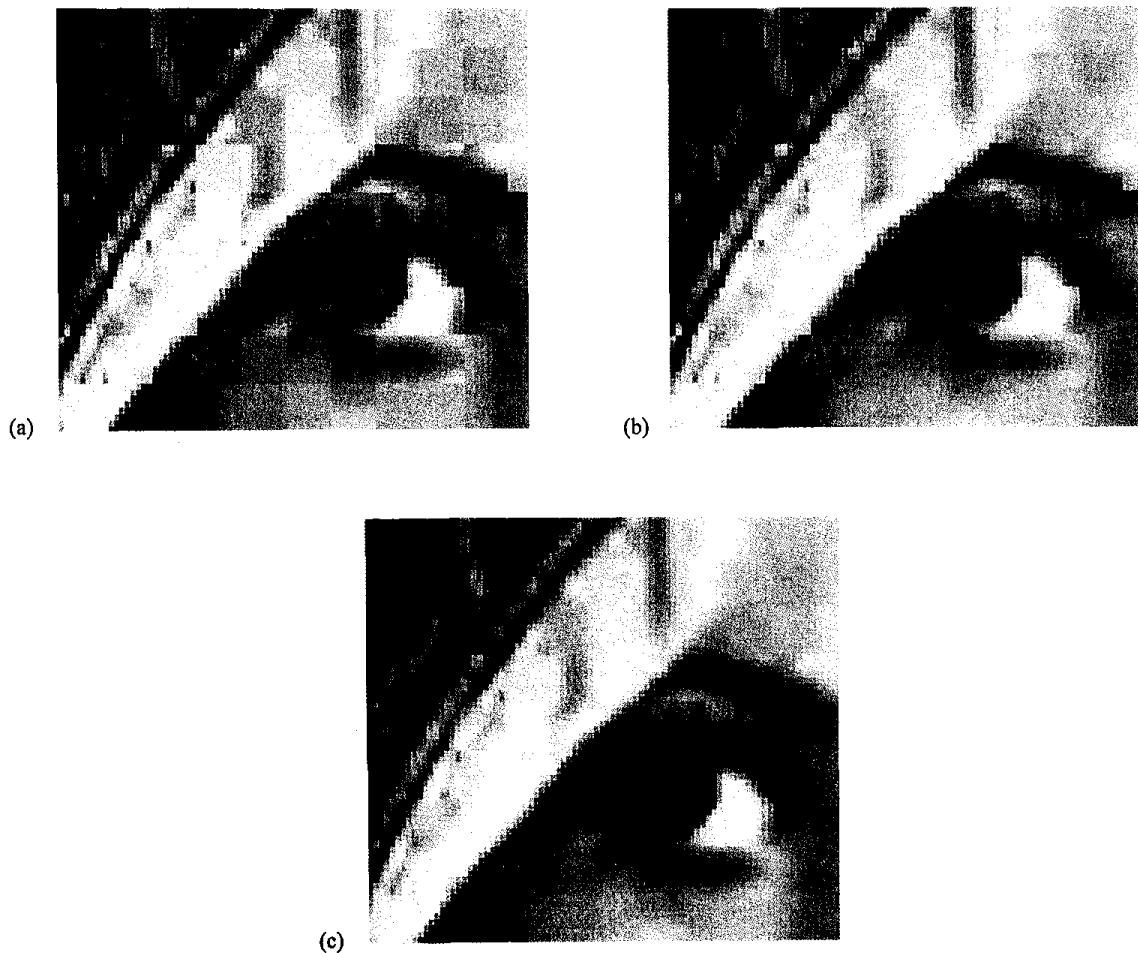


Figure 5: Demonstration of the proposed regularized dequantizer. (a) H.263+ decompressed image, (b) H.263+ decompression followed by the deblocking filter (Annex J) and (c) the decompressed image by the proposed regularized dequantizer.

In addition to the numerical improvements discussed above, the visual improvement offered by the proposed regularized dequantizer becomes apparent upon viewing the zoomed decompressed images. Figure 3 shows the original image (left), the image as decoded by the standard MPEG (center) and the image as decoded by the proposed dequantizer. Figure 3 (a), (b) and (c) show the three images for I-, P- and B-frames, respectively. All images are zoomed by a factor two. The visual improvement offered by the regularized dequantization is self-evident upon a quick comparison of these images, with the largest improvement seen for the I-frame.

The proposed algorithm is also applicable to H.26x video compression standard as the standard is also based on DCT transform coding. In particular, we focus on the most recent H.263+ standard. The performance of the proposed regularized dequantizer is evaluated and compared to the standard H.263+ with its standard quantization table with and without the deblocking filter (Annex J).

Figure 4 shows plots of the PSNR (a) and the BM (b) values as functions of the quantization scale factor (QUANT of H.263+) using the standard Lenna image. The proposed algorithm consistently provides higher PSNR and lower BM values for all values of QUANT. The readily recognizable trend is that larger the quantization step size (QUANT) and thus lower the bit-rate, higher the performance gain of the regularized dequantizer over the conventional dequantizer. All images were obtained (for the regularized approach) in two iterations.

As was the case for MPEG video shown previously, although improvements in actual PSNR values appear to be small (less than 1 dB), the visual improvement offered by the proposed regularized dequantizer becomes apparent upon viewing the zoomed images. In Figure 5, (a) shows the image as decoded by H.263+, (b) shows the H.263+ decompression followed by the deblocking filter (H.263+ Annex J), and (c) shows the decoded image by the proposed regularized dequantizer. All images are zoomed by a factor three. Again, the visual improvement offered by the regularized dequantization is self-evident upon a quick comparison of these images.

To summarize, the proposed algorithm consistently provides higher PSNR and lower BM values for all values of the bitrate. The readily recognizable trend is that lower the bitrate, higher the performance gain achieved by the proposed regularized dequantizer over the conventional decompression.

5. CONCLUSION

We have presented a new technique for decompressing DCT encoded images based on our proposed regularized dequantizer. The superiority of the proposed technique has been demonstrated over the existing MPEG as well as H.263+ standard with and without its deblocking filter. As simulations have indicated, the proposed technique would be particularly appropriate for low-bit rate videos.

ACKNOWLEDGEMENTS

This research was supported in part by the grant E-00261 (program year 1999-2000) from the Korea Research Foundation.

REFERENCES

- [1] Prost R, Ding Y. and Baskurt A., "JPEG dequantization array for regularized decompression", *IEEE Trans. on Image Proc.*, vol. 6, no. 6, pp. 883-888, June 1997.
- [2] Miller K., "Least squares methods for ill-posed problems with a prescribed bound", *SIAM J. Math. Anal.*, vol. 1, pp. 52-74, Feb. 1970.
- [3] Katsaggelos A. K., Biedmond J. Schafer R. W. and Mersereau R. M., "A regularized iterative image restoration algorithm", *IEEE Trans. on Signal Proc.*, vol. 39, pp. 914-929, Apr. 1991.
- [4] Philips W., "Correction to 'JPEG dequantization array for regularized decompression'", *IEEE Trans. on Image Proc.*, vol. 6, no. 6, pp. 883-888, 1997.
- [5] Konstantinides K. Bhaskaran V. and Beretta G., "Image sharpening in the JPEG domain", *IEEE Trans. on Image Proc.*, vol. 8, no. 6, June 1999.
- [6] Tikhonov A. N. and Arsenin V. Y., *Solutions of Ill-Posed Problems*. Washington DC: Winston and Sons, 1977.
- [7] Luenberger D. G., *Optimization by Vector Space Methods*. New York: John Wiley, 1969.
- [8] Song S. M., Napel S., Pelc N. J. and Glover G. H. "Phase unwrapping of MR phase images using Poisson equation", *IEEE Trans. on Image Proc.*, vol. 4, no. 5, May 1995.



Gunho Lee was born in Miryang, Korea, on July 6, 1975. He received the S.B. degree in Electrical Engineering at the Korea University, Seoul, Korea, in 1998. He is currently pursuing the S.M. degree in Electrical Engineering at the Korea University.

His current research interests include image processing, image data compression and specifically algorithms for image recovery/enhancement, analysis for multimedia applications, signal processing.



Sung-Jea Ko (M'88-SM'97) received the Ph.D. degree in 1988 and the M.S. degree in 1986, both in Electrical and Computer Engineering, from State University of New York at Buffalo, and the B.S. degree in Electronic Engineering at Korea University in 1980. In 1992, he joined the Department of Electronic Engineering at Korea University where he is currently a Professor. From 1988 to 1992, he was an Assistant Professor of Electrical and Computer Engineering at the University of Michigan-Dearborn. From 1981 to 1983, he was with Daewoo Telecom Corporation where he was involved in research and development on data communication systems.

He received the Hae-Dong best paper award from the Institute of Electronics Engineers of Korea (1997), and the best paper award from the IEEE Asia Pacific Conference on Circuits and Systems (1996). He is the 1999 Recipient of the LG Research Award given to the Outstanding Information and Communication Researcher. Dr. Ko is currently the Consumer Electronics chapter chairman of the IEEE Korea Council. His current research interests are in the areas of digital signal and image processing, and multimedia communications.



Sanghoon Sull received the B.S degree with honors in electronics engineering from the Seoul National University, Korea, in 1981, the M.S. degree in electrical engineering from the Korea Advanced Institute of Science and Technology, Korea, in 1983, and the Ph.D. degree in electrical and computer engineering from the University of Illinois, Urbana-Champaign, in 1993. From March 1983 to July 1986, he worked for the Korea Broadcasting Systems as a research and development engineer.

From March 1994 to July 1996, he conducted a research on video based obstacle detection at the NASA, Ames Research Center. From August 1996 to August 1997, he conducted a research on video indexing and retrieval and was involved in the development of the IBM DB2Video Extender at the IBM, Almaden Research Center. He joined the School of Electrical Engineering at the Korea University as an assistant professor in August 1997 and is now an associate professor. His current research interests include multimedia data management including indexing and retrieval, MPEG-7, image understanding and processing, and computer graphics.



S. Moon-Ho Song received the S.B. degree from the Massachusetts Institute of Technology in 1982, the M.S. degree from the University of California, Los Angeles, in 1985, and the Ph.D. degree from the University of Southern California in 1991, all in electrical engineering.

He was with Litton Guidance and Control Systems from 1982 to 1983, where he worked on developing various inertial navigation systems. From 1983 to 1991, he was a member of the technical staff at Hughes Aircraft Company, where he developed radar signal processing algorithms and software. From 1992 to 1993, he was a research associate at the Richard M. Lucas Magnetic Resonance Imaging and Spectroscopy, Stanford University, where he developed new image processing techniques for MR and CT applications. From 1994 to 1995, he served on the faculty of the Department of Radiology at the University of California, San Francisco. In 1995, he joined the faculty of the School of Electrical Engineering at Korea University, Seoul, Korea, where he is currently an associate professor. His current research interests include image processing and analysis for multimedia applications, numerical algorithms, signal processing, and non-destructive testing using tomography.

Dr. Song holds three patents and has several patents pending. He is a member of IEEE, IS&T, IEEK, KICS and Eta Kappa Nu.